Articles

Contribution from the Kenan Laboratories of Chemistry,
The University of North Carolina, Chapel Hill, North Carolina 27514

Oxidative Microelectrode Voltammetry of Tetraphenylporphyrin and Copper Tetraphenylporphyrin in Toluene Solvent

L. Geng and Royce W. Murray*

Received January 3, 1986

Vapor pressure osmometric, viscometric, and conductometric studies of 0.001–0.7 M tetrahexylammonium perchlorate (Hx_4NClO_4) solutions in toluene show that this electrolyte aggregates to trimers and tetramers even at very low concentrations and undergoes formation of higher organized structures $\{(Hx_4N)_n(ClO_4)_n\}$ beginning at about 0.1 M. The oxidative voltammetry of copper tetraphenylporphyrin (CuTPP) at 10-μm Pt microelectrodes shows a single two-electron wave at 0.1 M Hx_4NClO_4/toluene that becomes resolved into two one-electron waves at higher [Hx_4NClO_4]. Analysis of the [Hx_4NClO_4] dependency of the CuTPP oxidation waves shows that ClO_4^- axial coordination occurs to $CuTPP^+$ and $CuTPP^{2+}$ and that these cations become thereby drawn into the organized $\{(Hx_4N)_n(ClO_4)_n\}$ structures. A similar phenomenon occurs upon oxidation of the free-base porphyrin H_2TPP in Hx_4NClO_4/toluene. When trioctylphosphine oxide (TOPO) is present during H_2TPP oxidation, proton transfer occurs to the TOPO base, leaving a further oxidizable porphyrin. The overall reaction is an irreversible four-electron process in the presence of excess TOPO. The rate constant for proton loss from H_2TPP^{2+} was measured as 275 M^{-1} s^{-1}.

The investigation of electrochemical oxidations and reductions in very low dielectric solvents[1] and in other highly resistive media[2] has recently become feasible through the use of very small area electrodes (microelectrodes[3]). Currents that flow at microelectrodes are so small that the solvent need have only modest ionic conductivity, such as by dissolution of a dissociable electrolyte, in order to eliminate otherwise debilitating ohmic distortion of electrochemical responses. Tetrahexylammonium perchlorate (Hx_4NClO_4) has been used as an electrolyte in the solvents benzene[1b,c] and toluene,[1a] and a reference electrode potential scale has been developed for Hx_4NClO_4/toluene solutions.[1a]

We have been interested in exploiting microelectrode voltammetry to probe how electrochemical reactions, and the chemical reactions that are often coupled to them, are affected by the use of very low dielectric solvents. Potentially solvent-sensitive electrode reactions are in particular those that promote changes in the coordination shell of a metal complex and those leading to species with significant electrophilic, nucleophilic, or protonic acid–base reactivity. A solvent like toluene may evoke coupled electrode–chemical reaction pathways differing from those observable in more traditional solvents. The strategy of exploring new solvents has long been profitable in electrochemical studies;[4] a recent example was given by Sharp and Bard,[4b] who chose the difficulty oxidized SO_2 solvent medium to gain access to new electrochemistry and chemistry of highly oxidizing redox couples.

This paper describes enhanced axial coordination and acid–base chemistry that we have encountered in the oxidative electrochemistry of tetraphenylporphyrin (free-base form, H_2TPP) and of copper(II) tetraphenylporphyrin (CuTPP) in Hx_4NClO_4/toluene solvent. Our investigation of these particular porphyrins was aimed at understanding why in 0.2 M Hx_4NClO_4/toluene they are oxidized in a single two-electron wave.[1a] Sequential one-electron steps are more typical[5] for these and other simple metalloporphyrins in CH_2Cl_2 and other solvents. Probing the two-electron waves by adding various axially coordinating nitrogeneous bases to solutions of CuTPP and H_2TPP in Hx_4NClO_4/toluene proved unsuitable because of oxidation of the base either directly or via porphyrin mediation.[6] We found however that the simple step of using high Hx_4NClO_4 electrolyte concentrations (using elevated temperatures to promote solubility) resolved the two-electron steps into a pair of one-electron processes. This result in turn prescribed a need to characterize concentrated (0.1–0.7 M) Hx_4NClO_4/toluene electrolyte solutions, a brief study of which is reported here.

A second phenomenon encountered when the effects of potential axial bases were tested was that the two electron oxidation wave of H_2TPP in 0.2 M Hx_4NClO_4/toluene was enhanced to an apparent four-electron wave by the addition of small molar excesses of the weak base trioctylphosphine oxide (TOPO). This proved to be an example of acid–base chemistry promoted by the toluene medium.

Experimental Section

Chemicals and Electrodes. Reagent grade toluene solvent (Fisher Scientific) was distilled over P_2O_5. The tetrahexylammonium perchlorate supporting electrolyte (Alfa Products) was recrystallized twice from either methanol or ethylacetate. Trioctylphosphine oxide (Aldrich) was used as received. Microdisk electrodes were constructed as in a previous paper,[2b] by using 10- and 50-μm Pt from Goodfellow Metals and 70-μm Pt wire cut from a Pt gauze. All were polished with 0.05-μm alumina (Buehler) prior to each experiment. Porphyrins were obtained from Man-Win Chemicals (CuTPP) and Strem Chemicals (H_2TPP).

Measurements. Microelectrode voltammetry was carried out with a sensitive potentiostat[7] in conventional cells enclosed by a copper-mesh

---

(1) (a) Geng, L.; Ewing, A. G.; Jernigan, J. C.; Murray, R. W. *Anal. Chem.* **1986**, *58*, 852. (b) Howell, J. O.; Wightman, R. M. *J. Phys. Chem.* **1984**, *88*, 3915. (c) Lines, R.; Parker, V. D. *Acta. Chem. Scand., Ser. B* **1977**, *B31*, 309.

(2) (a) Bond, A. M.; Fleischmann, M.; Robinson, J. *J. Electroanal. Chem. Interfacial Electrochem.* **1984**, 168, 299. (b) Howell, J. O.; Wightman, R. M. *Anal. Chem.* **1984**, *56*, 524. (c) Ewing, A. G. Feldman, B. J.; Murray, R. W. *J. Phys. Chem.* **1985**, *89*, 1263. (d) Bond, A. M.; Fleischmann, M.; Robinson, J. *J. Electroanal. Chem. Interfacial Electrochem.* **1980**, *180*, 257.

(3) (a) Wightman, R. M. *Anal. Chem.* **1981**, *53*, 1125A. (b) Dayton, M. A.; Brown, J. C.; Stutts, K. J.; Wightman, R. M. *Anal. Chem.* **1980**, *52*, 946.

(4) (a) Mann, C. K.; Barnes, K. K. *Electrochemical Reactions in Nonaqueous Systems*; Marcel Dekker: New York, 1970. (b) Sharp, P. R.; Bard, A. J. *Inorg. Chem.* **1983**, *22*, 2689.

(5) (a) Dolphin, D., Ed. *The Porphyrins*; Academic: New York, Vol. V, Chapter 3, pp 53–126, Chapter 4, pp 127–150. (b) Bottomly, L. A.; Kadish, K. M. *Inorg. Chem.* **1981**, *20*, 1348. (c) Peychal-Heiling, G.; Wilson, G. S. *Anal. Chem.* **1971**, *43*, 550. (d) Giraudeau, A.; Callot, H. L.; Jordan, J.; Ezhar, D., Cross, M. *J. Am. Chem. Soc.* **1979**, *101*, 3857. (e) Wolberg, A.; Manassen, J. *J. Am. Chem. Soc.* **1970**, *92*, 2982. (f) Wolberg, A.; Manassen, J. *Inorg. Chem.* **1970**, *9*, 2365. (g) Felton, R. H.; Linschitz, H. *J. Am. Chem. Soc.* **1966**, *88*, 1113. (h) Kadish, K. M.; Morrison, M. M. *Bioinorg. Chem.* **1977**, *7*, 107. (i) Chang, D.; Malinski, T.; Ulman, A.; Kadish, K. M. *Inorg. Chem.* **1984**, *23*, 817.

(6) Kadish, K. M.; Rhodes, R. K. *Inorg. Chem.* **1980**, *20*, 2961.

(7) Ewing, A. G.; Dayton, M. A.; Wightman, R. M. *Anal. Chem.* **1981**, *53*, 1842.

0020-1669/86/1325-3115$01.50/0

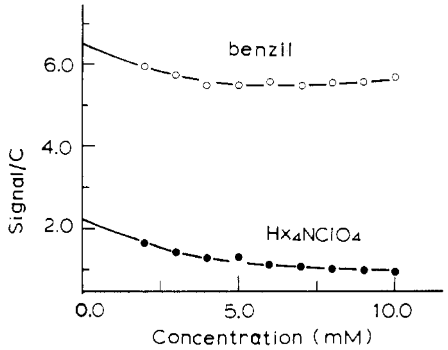

Figure 1. Concentration-normalized vapor pressure osmometric responses for benzil and Hx_4NClO_4 in toluene.

Faraday cage as described previously.[2b] Temperature control of the water bath in the Faraday cage was effected by circulating water from an external thermostated bath through a well-grounded loop of copper tubing. Conductivities of Hx_4NClO_4 solutions were measured by using two approaches: (i) a fixed frequency Industrial Conductivity Model E-362 bridge and conventional platinized Pt electrodes, and (ii) a ac impedance analysis of a 10-μm Pt microelectrode–Pt foil pair with a Solartron Model 1250 frequency response analyzer equipped with a Model 1186 electrochemical interface. Solution viscosities were measured with calibrated size 50 and 100 Cannon–Fenske capillary viscometers. Vapor pressure osmometry was performed with a Knauer Model 11.00 instrument.

Results and Discussion

Vapor Pressure Osmometry and Viscosity of Hx_4NClO_4/Toluene Solutions. At room temperature, the concentration range of Hx_4NClO_4 useable for 10-μm-microdisk voltammetry is narrow, bounded by excessive resistivity below ca. 0.05 M and by the ca. 0.1 M electrolyte solubility. The electrolyte solubility increases substantially with temperature; however, 0.7 M Hx_4NClO_4 readily dissolves in toluene at 45 °C. At this electrolyte concentration, the electrolyte comprises a 0.07 mole fraction of the solution and approximately 31% of the solution volume.

Previous vapor pressure osmometric and NMR-based studies[8] have shown that dilute solutions of alkylammonium salts (RNH_3X, where R is typically dodecyl) in low dielectric solvents (including benzene and toluene) undergo aggregation to trimer and higher order clusters. We applied vapor pressure osmometry to comparably low concentration Hx_4NClO_4/toluene solutions, with results as shown in Figure 1. By comparison to benzil as a nonassociating model compound, extrapolating the concentration-normalized instrument response to zero concentration gives an apparent 3-fold enhanced molecular weight of Hx_4NClO_4 units. The result means that this salt aggregates, at very low concentrations, into trimers

$$3Hx_4NClO_4 \rightleftarrows (Hx_4N)_3(ClO_4)_3 \qquad (1)$$

At higher [Hx_4NClO_4] concentrations in Figure 1, the osmometric response relative to benzil steadily decreases until at 10 mM Hx_4NClO_4, it appears that a significant fraction of the electrolyte has further aggregated into a tetrameric form.

The results of extending the 45 °C vapor pressure osmometric measurements into a higher, electrochemically useable range of Hx_4NClO_4 concentrations are shown in Figure 2B. In the left-hand, lower concentration portion of these data, the apparent molecular weight of Hx_4NClO_4 continues to increase steadily, consistent with continued formation of higher aggregates. The distinctive aspect of Figure 2B, is, however, the fairly abrupt minimum observed at about 0.1 M Hx_4NClO_4. This minimum clearly signals a basic change in the manner in which the Hx_4NClO_4 units are associated.

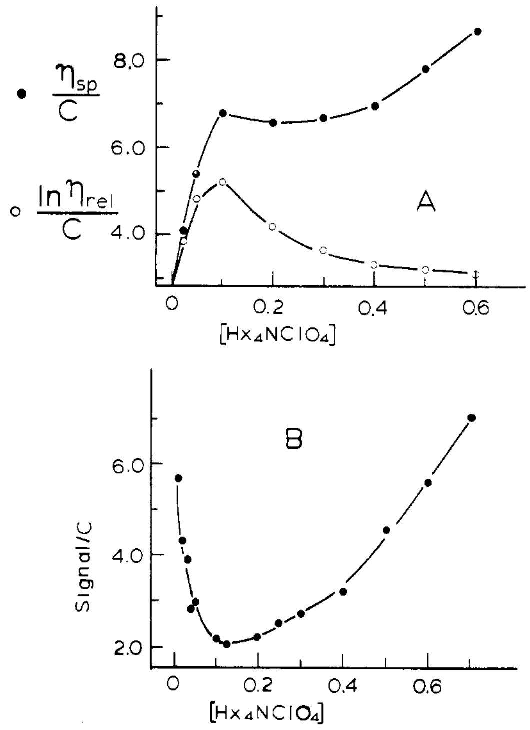

Figure 2. Concentration-normalized viscosities (A) and vapor pressure osmometric responses (B) for Hx_4NClO_4 in toluene.

That there is some change in the Hx_4NClO_4 association behavior at 0.1 M Hx_4NClO_4 is reinforced by the 45 °C viscosity data shown in Figure 2A. The specific viscosities show an even more abrupt change at ca. 0.1 M Hx_4NClO_4.

We believe it is reasonable to interpret the osmometric and viscosity data of Figure 2 in terms of higher organized structures or clusters of Hx_4NClO_4 units that begin to form at about 0.1 M concentration. Formation of inverted micelles in nonpolar solvents (ionic groups in the interior cavity and hydrocarbon groups extending into bulk nonpolar solvent) has indeed been reported for RNH_3X alkylammonium salts[8] in benzene. The critical micelle concentrations (cmc) for the earlier reports are all much lower (0.001–0.01 M) than in the present case. The previous data were all, however, for *mono*alkylammonium salts and at lower temperatures. We infer that formation of higher organized structures in toluene by the *tetra*alkylammonium salt Hx_4NClO_4 is a considerably less favorable process. Further, the organized Hx_4NClO_4 structures may, because of the symmetrically substituted cation, involve less distinctly defined ionic regions and nonpolar bulk solvent regions than, for example, would be imagined for inverted dodecylammonium butyrate micelles in benzene. In other words, it is not obvious that higher organized Hx_4NClO_4 structures in toluene should be viewed as micelles. Additionally, the higher organized Hx_4NClO_4 structures may incorporate an appreciable amount of toluene solvent, judging from the fact that the normally large toluene solubility of CuTPP decreases appreciably in 0.5–0.7 M electrolyte.

Conductivity of Hx_4NClO_4/Toluene Solutions. Tetraalkylammonium salt solutions employed in electrochemical experiments in solvents like H_2O, CH_3CN, and CH_2Cl_2 are usually extensively or completely dissociated, and their ionic contents are regarded as equal to the electrolyte concentration. This is not the case with Hx_4NClO_4 in toluene. The conductivity of 45 °C Hx_4NClO_4/toluene solutions changes nonlinearly with concentration, as shown by the log–log plots in Figure 3. Conductivities (●) measured with a conventional conductivity bridge give a log–log slope of 2.1, meaning that conductivity varies with $[Hx_4NClO_4]^{2.1}$. Conductivities measured (○) with a more exacting combination of a 10-μm Pt microelectrode, an ac impedance analysis to separate

---

[8] (a) David-Auslaender, J.; Gutmann, H.; Kertes, A. S.; Zanger, M. *J. Solution Chem.* **1974**, *3*, 251. (b) Lo, F. Y.-F.; Escott, B. M.; Fendler, E. J.; Adams, E. T.; Larsen, R. D.; Smith, P. W. *J. Phys. Chem.* **1975**, *79*, 2609. (c) Fendler, J. H. *Membrane Mimetic Chemistry*; Wiley: New York, 1982; Chapter 3, p 48. (d) Fendler, J. H.; Fendler, E. J.; Medary, R. T.; El Seound, O. A. *J. Chem. Soc., Faraday Trans. 1* **1973**, *69*, 280. (e) Muller, N. *J. Phys. Chem.* **1975**, *79*, 287. (f) Fendler, E. J.; Fendler, J. H.; Medary, R. T.; El Seound, O. A. *J. Phys. Chem.* **1973**, *77*, 1432. (g) El Seound, O. A.; Fendler, E. J.; Fendler, J. H.; Medary, R. T. *J. Phys. Chem.* **1973**, *77*, 1876.

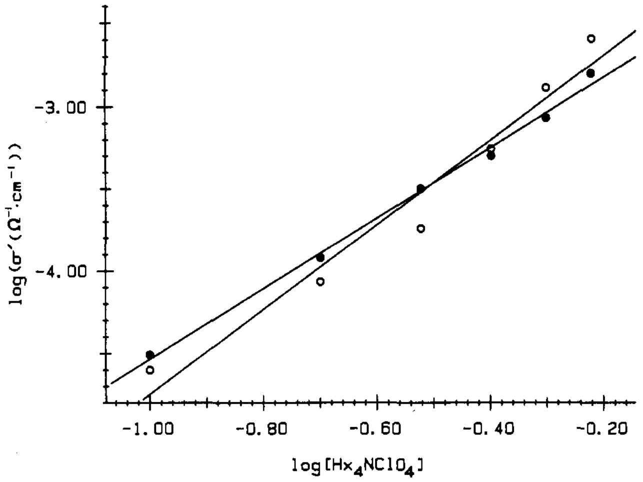

Figure 3. Logarithmic plots of conductivity as determined by a fixed-frequency bridge (●) and by an ac-impedance method varying frequency to produce a totally in-phase impedance (○). In both cases conductivity is corrected for viscosity by multiplying by the ratio of viscosity at the given $[Hx_4NClO_4]$ to that at 0.1 M, all at 45 °C.

resistance and capacitance contributions, and Newman's theory,[9] give similar values, but the log–log slope (average 2.5) gradually increases at higher concentrations. Both plots are given as conductivity–viscosity products (σ') to correct for viscosity-associated changes in ionic diffusion coefficients (which by the Stokes–Einstein equation[10] are inversely proportional to viscosity). Variation of conductivity with $[Hx_4NClO_4]^2$ would be consistent with charge-separating ion pair dissociation from tetrameric aggregates

$$(Hx_4N)_4(ClO_4)_4 \rightleftarrows [(Hx_4N)_4(ClO_4)_3]^+ + ClO_4^- \qquad (2)$$

or alternatively

$$(Hx_4N)_4(ClO_4)_4 \rightleftarrows [(Hx_4N)_3(ClO_4)_4]^- + Hx_4N^+ \qquad (3)$$

The increase in slope of the ac impedance data (Figure 3) suggests that actually the average size of the aggregate from which dissociation occurs gradually increases with concentration, which is consistent with the results of Figure 2. The situation is additionally complicated by the possibility of alternative charge-separating mechanisms based on dissociation of the organized structures into ionic monomers or ionic clusters, such as

$$(Hx_4N)_n(ClO_4)_n \rightleftarrows [(Hx_4N)_{n-x}(ClO_4)_{n-y}]^{y-x} + [(Hx_4N)_x(ClO_4)_y]^{x-y} \qquad (4)$$

where x and y might vary. In either case it is important to note that Figure 3 reflects only the concentration of dissociated (charge separated) and thus current-carrying ionic species. Solvent-separated but not dissociated ion pairs should not contribute to solution conductivity[11] nor should dissociations of ion pairs in which both ions *remain* in the same (and thus overall electroneutral) aggregate or micelle. Thus, dissociations of a Hx_4NClO_4 ion pair that is a *constituent* of a Hx_4NClO_4 tetramer (or of a higher organized structure)

$$(Hx_4N)_n(ClO_4)_n \rightleftarrows \{(Hx_4N^+),(Hx_4N)_{n-1}(ClO_4)_{n-1},(ClO_4^-)\} \qquad (5)$$

with retention of both dissociated Hx_4N^+ and ClO_4^- species *within* the aggregate, would not be measured by the conductivity data of Figure 3. This observation is important in considering the effect of the concentration of (Hx_4NClO_4) electrolyte on CuTPP electrochemistry; see below.

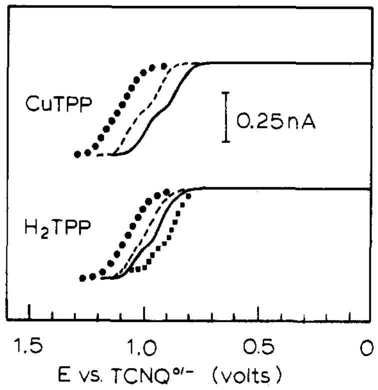

Figure 4. Microelectrode voltammograms at different $[Hx_4NClO_4]$ for CuTPP [(●) 0.1 M; (---) 0.3 M; (—) 0.6 M] and for H_2TPP [(●) 0.2 M; (---) 0.4 M; (—) 0.6 M, (■) 0.7 M) in toluene at 45 °C, using 10 μm diameter Pt electrodes.

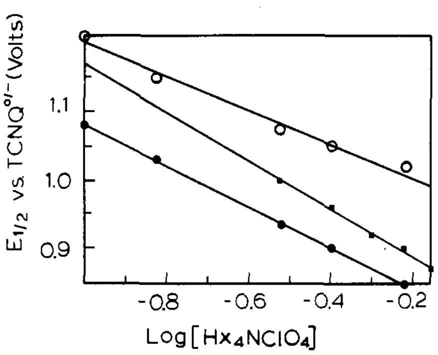

Figure 5. Plot of $E_{1/2}$ of microelectrode voltammograms of Figure 4 (and others not shown there) against $[Hx_4NClO_4]$ in toluene at 45 °C: (●) $CuTPP^{0/+}$ (30-mV slope); (○) $CuTPP^{+/2+}$ (24-mV slope); (■) $H_2TPP^{0/+}$ (35-mV slope).

This brief study of aggregation and conductivity shows that Hx_4NClO_4/toluene solutions are probably more complex electrochemical reaction media than say, Et_4NClO_4 in acetonitrile. On the other hand, there have been several reports[12] of readily understandable electrochemical reactions in aqueous solutions containing organized electrolyte structures, so the presence of micellar structures is not necessarily undesirable. Also, the results clearly show that Hx_4NClO_4/toluene solutions should not be considered as diluted "molten salts".

Microelectrode Voltammetry of H_2TPP and CuTPP Solutions. Microelectrode oxidations of these porphyrins and of NiTPP in 0.1 M Hx_4NClO_4/toluene solutions give single oxidation waves that, upon comparison to the currents observed for the $Por^{0/-}$ reduction couples, are clearly two-electron steps at both room temperature[1a] and 45 °C. At higher $[Hx_4NClO_4]$ and 45 °C, the two-electron waves split into two waves of generally equal height as shown in Figure 4. Using the $E_{1/2}$ of the reduction wave of added tetracyanoquinodimethane ($TCNQ^{0/-}$) as a reference potential[1a] establishes that both waves shift negatively at higher $[Hx_4NClO_4]$, and their separation occurs because the first porphyrin oxidation $E_{1/2}$ shifts somewhat more than does that of the second oxidation step.

An analysis of the variation of $E_{1/2}$ for the two CuTPP steps (Figure 5) shows that the $E_{1/2}$ values of both porphyrin waves change with $[Hx_4NClO_4]$ in a Nernstian manner according to the relation

$$E = \text{constant} - 0.063 \log [Hx_4NClO_4]^x \qquad (6)$$

---

(9) Newman, J. *J. Electrochem. Soc.* **1966**, *113*, 501.

(10) Atkins, P. W. *Physical Chemistry*, p. 905, W. H. Freeman & Company, San Francisco, 1982.

(11) Fuoss, R. M. *J. Phys. Chem.* **1978**, *82*, 2427.

(12) (a) Franklin, T. C.; Iwunze, M. *Anal. Chem.* **1980**, *52*, 973. (b) Ohsawa, Y.; Aoyagui, S. *J. Electroanal. Chem. Interfacial Electrochem.* **1982**, *136*, 353. (c) Hayano, S.; Shinozuka, N. *Bull. Chem. Soc. Jpn.* **1969**, *42*, 1469. (d) *Ibid.* **1970**, *43*, 2083. (e) *Ibid.* **1971**, *44*, 1503. (f) Suzuki, H.; Shinozuka, N.; Hayano, S. *Bull. Chem. Soc. Jpn.* **1974**, *47*, 1093. (g) Yeh, P.; Kuwana, T. *J. Electrochem. Soc.* **1976**, *123*, 1334. (h) Kaifer, A. E.; Bard, A. J. *J. Phys. Chem.* **1985**, *89*, 4876.

where the multiplier of the log term is the appropriate Nernstian one for 45 °C. The slopes for the $CuTPP^{+/0}$ and $CuTPP^{2+/+}$ plots are 30 and 24 mV, corresponding to $x = 0.5$ and 0.4, respectively.

The results of Figure 4 and 5 show that some component of the Hx_4NClO_4 electrolyte participates in the electrode reaction. The direction of the $E_{1/2}$ shifts could come about either by associative interaction between oxidized metalloporphyrins and ClO_4^- or between reduced $TCNQ^-$ and Hx_4N^+. The latter interaction should be weak compared to the former one, and additionally would not account for $E_{1/2}$ shifting differently for the $CuTPP^{0/+}$ and $CuTPP^{+/2+}$ reactions. The vis-UV spectrum of CuTPP in toluene is unchanged by addition of 0.6 M Hx_4NClO_4, so interactions of ClO_4^- with unoxidized metalloporphyrin seem minor or absent. The main effect is therefore a stabilizing, axially ligating interaction of ClO_4^- with the cationic, oxidized forms of the metalloporphyrin. This is unsurprising given the previous crystallographic and spectroelectrochemical studies that have established axial perchlorate binding to the cation radical of ZnTPP[13] and to $Fe^{III}TPP$,[14] respectively. Finally, since the $E_{1/2}$ values of both CuTPP oxidation waves vary with $[Hx_4NClO_4]$, each of the two oxidation steps must involve some change in the number of bound ClO_4^- species, which suggests the following scheme for the CuTPP microelectrode voltammetry

$$CuTPP \xrightarrow{-e^-} CuTPP^+ \xrightarrow{L} (CuTPP^+)(L) \xrightarrow{-e^-} (CuTPP^{2+})(L) \xrightarrow{L} (CuTPP^{2+})(L)_2 \quad (7)$$

in which L represents a source of an axially binding ClO_4^- from the electrolyte.

It remains now to accomodate the identity of L to the results of Figure 5. If L were solely ClO_4^- dissociated from tetrameric aggregates according to eq 2, then in eq 6 x should be 2.0. The experimental results for x from Figure 5 are however near 0.5, meaning that, for both CuTPP oxidations in eq 7, the concentration of the active binding species varies with the square root of the Hx_4NClO_4 concentration. This concentration dependency suggests that L is derived from dissociation of *monomeric* Hx_4NClO_4 units. Monomeric Hx_4NClO_4 units are however not revealed at all by the osmometric results, which show clearly that, even at very low Hx_4NClO_4 concentrations, Hx_4NClO_4 remains as an aggregated cluster.

The apparent inconsistency is resolved by reference to eq 5, in which the dissociation of Hx_4NClO_4 units *within* tetramers or higher organized structures causes $[ClO_4^-]$ to vary with the square root of the overall Hx_4NClO_4 concentration. The importance of this interpretation is that the axial binding of $CuTPP^+$ and $CuTPP^{2+}$ occurs with ClO_4^- remaining *within* the aggregate or higher organized structure; that is, the oxidation of CuTPP to its radical cation may be represented by

$$\{(Hx_4N^+),(Hx_4N)_{n-1}(ClO_4)_{n-1},(ClO_4^-)\} + CuTPP \xrightarrow{-e^-} \{(Hx_4N^+),(Hx_4N)_{n-1}(ClO_4)_{n-1},(CuTPP^+ClO_4^-)\}^+ \quad (8)$$

The oxidized metalloporphyrin is thereby drawn into the higher organized structure. Similarly, oxidation of the CuTPP radical cation to its dication may be represented by

$$\{(Hx_4N^+),(Hx_4N)_{n-1}(ClO_4)_{n-1},(CuTPP^+ClO_4^-)\}^+ \xrightarrow{-e^-} \{(Hx_4N^+)_2,(Hx_4N)_{n-2}(ClO_4)_{n-2},(ClO_4^-CuTPP^{2+}ClO_4^-)\}^{2+} \quad (9)$$

This proposal has precedent in the electrochemical-micelle literature; Blount, et al.[15] have described a micelle-enhanced ion pairing phenomenon in which nitrobenzene radical anions are incorporated into a cationic micellar pseudophase.

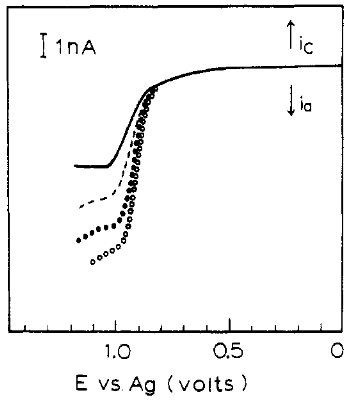

Figure 6. Microelectrode voltammograms of 0.34 mM H_2TPP at a 50 μm diameter Pt electrode in 0.2 M Hx_4NClO_4/toluene at 30 °C with (—) 0 M, (---) 1.3 mM, (●) 6.0 mM, and (○) 13.9 mM TOPO.

The microelectrode voltammetry of H_2TPP responds to varying $[Hx_4NClO_4]$ in a manner generally similar to that of CuTPP. The slope of the Figure 4 Nernstian plot corresponds to $x = 0.55$ for the $H_2TPP^{+/0}$ couple. In this case axial binding of L can be considered as an acid–base process where perchlorate is the base:

$$H_2TPP \xrightarrow{-e^-} H_2TPP^+ \xrightarrow{L} (H_2TPP^+)(L) \xrightarrow{-e^-} (H_2TPP^{2+})(L) \quad (10)$$

Again, by analogy to our discussion of the CuTPP oxidation, we propose that the acid–base association with ClO_4^- occurs within the micellar phase. The analysis of the second oxidation step of H_2TPP is left incomplete because, in addition to a shift of $E_{1/2}$, its limiting current for unclear reasons decreases at high $[Hx_4NClO_4]$ (Figure 4).

One further point can be drawn from the data of Figure 4. It is clear that at low Hx_4NClO_4 electrolyte concentrations, the $E_{1/2}$ for the two oxidation steps for nonaxially coordinated CuTPP and for H_2TPP are quite similar in toluene, whereas in CH_2Cl_2 these potentials differ by 260 and 250 mV, respectively. The Hx_4NClO_4/toluene solvent medium seems to particularly stabilize the dicationic CuTPP and H_2TPP porphyrins relative to their monocations. It is plausible that this effect arises from a combination of the strongly ionic environment offered the dication in eq 9 and of the aromatic ring-solvating characteristics of toluene that is present in the structure.

Oxidation of H_2TPP in the Presence of Trioctylphosphine Oxide. Trioctylphosphine oxide (TOPO) is a convenient weak base reagent in toluene, being quite soluble and not readily oxidized at Pt microelectrodes. Judging from the absence of UV–vis spectral changes upon addition of >10× molar excesses of TOPO to H_2TPP solutions, interactions between H_2TPP and TOPO are weak or absent. Electrooxidized forms of H_2TPP do react with TOPO, however, in a manner different from that (Figure 4) with high concentrations of Hx_4NClO_4 electrolyte. Figure 6 shows how the single unresolved two-electron microelectrode voltammogram of H_2TPP (—) in 0.2 M Hx_4NClO_4 is changed in the presence of 3.8, 18, and 41 molar excesses of TOPO. A single voltammetric step is observed in all cases, and the limiting current increases from the two-electron value to, at high molar excesses of TOPO, that of a *four*-electron oxidation wave. The four electron oxidation is chemically irreversible; no rereduction wave appears under cyclic voltammetric conditions (70-μm Pt microelectrode and fast potential sweep rates) where a nearly fully developed two-electron rereduction wave for H_2TPP^{2+} is observable[1a] in the absence of TOPO.

Addition of TOPO to H_2TPP solutions in toluene that contain a large concentration of Hx_4NClO_4 electrolyte (so that the $H_2TPP^{+/0}$ and $H_2TPP^{2+/+}$ waves are distinguishable) causes an increase in the limiting current of the first oxidation wave. Thus, TOPO is reactive with H_2TPP^+ as well as with the H_2TPP^{2+} dication. A similar but less pronounced reactivity can be observed in CH_2Cl_2 solvent. In Bu_4NClO_4/CH_2Cl_2, H_2TPP exhibits at 10-μm Pt electrodes two well-resolved, one-electron-oxidation waves. These two waves are unaffected by addition of small amounts of TOPO, but larger excesses of TOPO cause an increase

---

(13) Spaulding, L. D.; Eller, P. G.; Bertrand, J. A.; Felton, R. H. *J. Am. Chem. Soc.* **1974**, *96*, 982.

(14) Kadish, K. M., Rhodes, R. K. *Inorg. Chem.* **1983**, *22*, 1090.

(15) McIntire, G. L.; Chiappardi, D. M.; Casselberry, R. L.; Blount, H. L. *J. Phys. Chem.* **1982**, *86*, 2632.

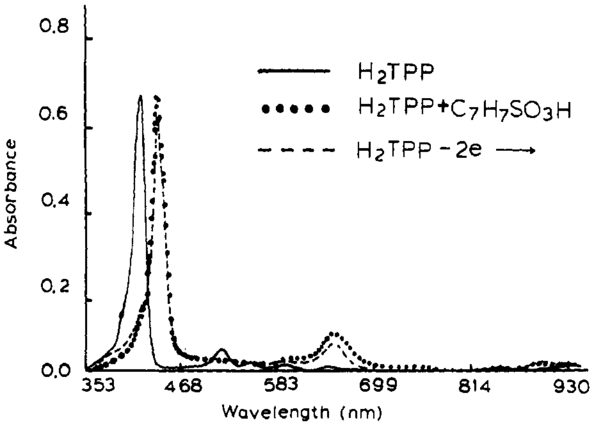

Figure 7. Spectra of H_2TPP in Bu_4NClO_4/CH_2Cl_2 solutions (–), after exhaustive oxidation on the plateau of the second voltammetric wave (---), and after addition of excess tosylic acid to a H_2TPP solution to prepare the H_4TPP^{2+} dication (●). All curves are obtained at the same initial H_2TPP concentration.

in current of the first oxidation wave just as in toluene.

We do not yet have in hand suitable experimental procedures for exhaustive electrolyses or spectroelectrochemistry of H_2TPP in toluene, and so have not been able to ascertain the nature of the final product(s) of the four-electron H_2TPP/TOPO reaction. However, parallel bulk electrolysis experiments in CH_2Cl_2 provide some important insights into the probable initial stages of the H_2TPP/TOPO reaction. Bulk electrolytic oxidation of a Bu_4NClO_4/CH_2Cl_2 solution (—) containing H_2TPP (and no TOPO) at a larger electrode, at a potential on the plateau of the second oxidation wave, leads upon partial oxidation (---) to appearance of the UV–vis spectrum in Figure 7 and eventual passage of 1.5–1.7 equivalents of charge. The new band appearing in Figure 7 has a λ_{max} identical to that of the core-protonated H_4TPP^{2+} species,[16] which is preparable (●) by addition of a small amount of strong acid to a H_2TPP solution. Voltammetry of such H_4TPP^{2+} solutions shows that this species is not oxidizable at accessible potential limits in either CH_2Cl_2 or toluene.

The inference that can be drawn from the above results is that on the slower times scale of a bulk electrolysis in CH_2Cl_2, the H_2TPP^{2+} dication is a sufficiently strong acid, and unoxidized H_2TPP is sufficiently basic, for proton transfer to occur during the electrolysis

$$H_2TPP^{2+} + H_2TPP \rightarrow (:)TPP + H_4TPP^{2+} \qquad (11)$$

where (:)TPP is a mono- or bis-deprotonated state that is readily further oxidized. Apparently the charge passed by further oxidation of (:)TPP approximately compensates for formation of the electro-inactive H_4TPP^{2+}, so that n remains near 2.

Significantly, if the electrolysis of H_2TPP in CH_2Cl_2 is repeated in the presence of a 10-fold excess of TOPO, the H_4TPP^{2+} spectral band is not as prominent and a larger number of equivalents (2.5) is passed. Thus, even in CH_2Cl_2, TOPO is a sufficiently strong base to compete with H_2TPP in eq 11, forming thus more (:)TPP and less H_4TPP^{2+}.

With the above observations in mind, the following scheme is proposed for the four electron oxidation of H_2TPP in toluene in the presence of TOPO

$$H_2TPP \xrightarrow{-2e^-} H_2TPP^{2+} \qquad (12)$$

$$H_2TPP^{2+} + TOPO \xrightarrow{k'} HTPP^+ + HTOPO^+ \qquad (13)$$

$$HTPP^+ \xrightarrow{-e^-} \xrightarrow{TOPO} \xrightarrow{-e^-} \text{products} \qquad (14)$$

where eq 12 and 13 and the first electron-transfer step in eq 14 represent an electrochemical "ECE" reaction sequence. This sequence is analogous to those commonly observed when radical anions are electrochemically produced in the presence of proton sources and when radical cations are electrochemically produced in the presence of nucleophiles.[17] We shall show next that the electrochemical data fit the behavior expected of an "ECE" reaction sequence, and allow an estimation of the rate constant for eq 13.

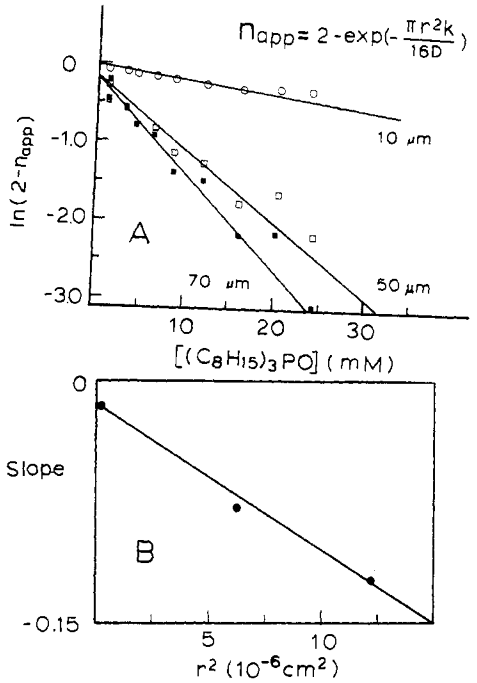

Figure 8. A. Plot of eq 16 for data taken with three microelectrodes of different radii, where k is proportional to [TOPO]. B. Plot of the slopes in part A vs. the squares of the microelectrode radii.

Comparison of limiting currents at 10, 50, and 70 μm diameter Pt microdisks shows that the Figure 6 transition from a two- to a four-electron oxidation of H_2TPP requires a considerably larger molar excess of TOPO when the smaller microelectrodes are used. This is qualitatively expected, since at the smaller microelectrode the rate at which H_2TPP^{2+} diffuses out of the diffusion layer around the microdisk electrode is accelerated relative to the rate at which further oxidizable porphyrin is generated by eq 13. The depth of the diffusion layer at a microelectrode decreases with electrode radius according to

$$\delta = \pi r/4 \qquad (15)$$

This equation is based on the Nernst diffusion layer treatment which is well-known to be a good approximation of rigorous mass transport theory.[18] Dayton, et al.[19] have made a similar observation on the relation between microelectrode radius and catalytic currents.

Two forms of "ECE" theory were compared to the microelectrode limiting currents for H_2TPP oxidation and their dependency on TOPO concentration. One theory is based on analogy to that of Adams et al.,[20] who related diffusion layers in chronoamperometry to those in rotated disk voltammetry (a steady-state experiment analogous to microelectrodes). We identify the time $t' = (\delta')^2/\pi D$ required for the diffusion layer at a *macro*electrode to grow to the dimensions δ of the *micro*electrode diffusion layer (eq 15). This time, $t' = \pi r^2/16D$, is substituted into the

---

(16) (a) Abraham, R. J.; Hawks, G. E.; Smith, K. M. *Tetrahedron Lett.* **1974**, 71. (b) Stone, A.; Fleischer, E. B. *J. Am. Chem. Soc.* **1968**, *90*, 2735.

(17) Bazier, M. M.; Lund, H. *Organic Electrochemistry*; Marcel Dekker: New York, 1983.

(18) Bard, A. J.; Faulkner, L. F. *Electrochemical Methods*; Wiley: New York, 1980; p 34.

(19) Dayton, M. A.; Ewing, A. G.; Wightman, R. M. *Anal. Chem.* **1980**, *52*, 2392.

(20) Malachesky, P. A.; Marcoux, L. S.; Adams, R. N. *J. Phys. Chem.* **1966**, *70*, 4068.

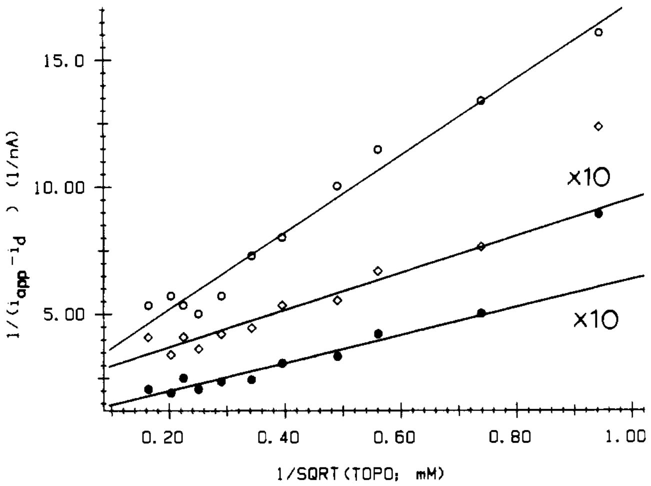

Figure 9. Plot of eq 18 for same data as used in Figure 8A. Electrode diameter: (○) 10 μm; (◇) 50 μm; (●) 70 μm.

chronoamperometric equation[20] for the "ECE" case to yield, after rearrangement

$$\ln [2 - n_{app}] = \pi r^2 k / 16D \qquad (16)$$

where n_{app} is the ratio of the microelectrode limiting current measured in the presence of TOPO to that measured (two-electron wave) in its absence, r is the microelectrode radius, D is the diffusion coefficient of H_2TPP, and k, the pseudo-first-order rate constant for eq 13, is equal to k'[TOPO] where k' is the second-order constant.

Figure 8A shows that microelectrode currents at 10-, 50-, and 70-μm microelectrodes, expressed as n_{app}, vary linearly with [TOPO] in the manner expected from eq 16. Figure 8A is equivalent to showing that the rate of the chemical step (eq 13) in the "ECE" scheme is first order in both H_2TPP and TOPO. Figure 8B demonstrates furthermore that the slopes of the plots in Figure 8A vary with the square of the microelectrode radius, as expected from eq 16. The slope of Figure 8B gives an estimate of the second-order rate constant k' of eq 13 as 275 M^{-1} s^{-1}. According to eq 13, this represents the rate constant for the extraction of a proton from the cation H_2TPP^{2+} by the phosphine oxide functionality.

The second theoretical analysis is based on ECE theory devised by Fleischmann et al.[21] for a microdisk electrode from microspherical electrode theory

$$[n_{app} - n_1]^{-1} = 4D^{1/2}/\pi r n_2 k^{1/2} + 1/n_2 \qquad (17)$$

where n_1 and n_2 are the numbers of electrons transferred prior to (eq 12 in our case) and after (eq 14) the chemical step and k is k'[TOPO]. By substituting the relation $n = i/4rFDC$, we obtain

$$[i_{app} - i_d]^{-1} = [\pi r^2 FCD^{1/2} k^{1/2}]^{-1} + [4n_2 rFDC]^{-1} \qquad (18)$$

where i_{app} and i_d are microelectrode currents in the presence and absence of TOPO, respectively.

Plots of $[i_{app} - i_d]^{-1}$ vs. $[TOPO]^{1/2}$ for the three sets of microelectrode data ($2r$ = 10, 50, 70 μm) are quite linear (Figure 9), in accord with eq 18. Their slopes, $[\pi r^2 FCD^{1/2} k^{1/2}]^{-1}$, vary with r^2 as predicted (plot similar to that shown in Figure 8B) and give an average rate constant k' = 308 M^{-1} s^{-1} for eq 13. This is in excellent agreement with the analysis of eq 16, considering the very different theoretical approaches.

Finally, note that the above analyses are based on using n_1 = 2 (i.e., eq 12). The data do not fit either theory for n_1 = 1. Thus, although TOPO is capable of reacting both with the cation radical H_2TPP^+ and the dication H_2TPP^{2+} (vide supra), the data in Figures 8 and 9 were collected at potentials where the rate of oxidation of H_2TPP^+ to H_2TPP^{2+} is much greater than the rate of reaction of H_2TPP^+ with TOPO. This forces the reaction into the scheme given as eq 12–14.

Conclusions

These microelectrode results show that the low dielectric Hx_4NClO_4/toluene medium does enhance ligand and acid–base reactivities sufficiently and on time scales so as to become revealed as new reactions coupled to heterogeneous electron-transfer events. Both reactions that we have studied in Hx_4NClO_4/toluene, that of coordination by ClO_4^- to H_2TPP and CuTPP and that of reaction of H_2TPP^{2+} with TOPO, are not apparent on microvoltammetric time scales in the more common CH_2Cl_2 solvent. In this sense, using the microelectrode strategy as a means of access to low dielectric media also has the value of serving as an access to both new electrochemical and new chemical reactions. Further studies of electrochemical and coupled chemical reactions in such media consequently seem worthwhile.

Acknowledgment. This research was supported in part by a grant from the National Science Foundation. We are grateful to R. P. Buck (UNC) for helpful discussions and use of the Solartron equipment and to M. Wightman (Indiana) and M. Fleischmann (Southampton) for helpful discussions on ac impedance and ref 21, respectively.

---

[21] Fleischmann, M.; Lasserre, F.; Robinson, J. *J. Electroanal. Chem. Interfacial Electrochem.* **1984**, *177*, 115.